

Partial Gromov-Wasserstein with Applications on Positive-Unlabeled Learning

Laetitia Chapel¹ Mokhtar Z. Alaya² Gilles Gasso³

Abstract

Optimal Transport (OT) framework allows defining similarity between probability distributions and provides metrics such as the Wasserstein and Gromov-Wasserstein discrepancies. Classical OT problem seeks a transportation map that preserves the total mass, requiring the mass of the source and target distributions to be the same. This may be too restrictive in certain applications such as color or shape matching, since the distributions may have arbitrary masses or that only a fraction of the total mass has to be transported. Several algorithms have been devised for computing unbalanced Wasserstein metrics but when it comes with the Gromov-Wasserstein problem, no partial formulation is available yet. This precludes from working with distributions that do not lie in the same metric space or when invariance to rotation or translation is needed. In this paper, we address the partial Gromov-Wasserstein problem and propose an algorithm to solve it. We showcase the new formulation in a positive-unlabeled (PU) learning application. To the best of our knowledge, this is the first application of optimal transport in this context and we first highlight that partial Wasserstein-based metrics prove effective in usual PU learning settings. We then demonstrate that partial Gromov-Wasserstein metrics is efficient in scenario where point clouds come from different domains or have different features.

1. Introduction

Optimal transport (OT) has been gaining in recent years an increasing attention in the machine learning community. This success is due to its capacity to exploit the geometric property of the samples at hand. Generally speaking, OT

is a mathematical tool to compare distributions by computing a transportation mass plan from a source to a target distribution. Distances based on OT are referred to as the Monge-Kantorovich or Wasserstein distances (Monge, 1781; Kantorovich, 1942; Villani, 2009) and have been successfully employed in a wide variety of machine learning applications including clustering (Ho et al., 2017), computer vision (Bonneel et al., 2011; Solomon et al., 2015), generative adversarial networks (Arjovsky et al., 2017) or domain adaptation (Courty et al., 2017). A key limitation of Wasserstein distance is that it relies on the assumption of aligned distributions, namely they belong to the same ground space or that a least a meaningful distance across domains can be computed. Nevertheless, source and target distributions can be collected under distinct environments, representing different times of collection, contexts or measurements (see Fig. 1, left). To get benefit from OT on such heterogeneous distribution settings, one can compute Gromov-Wasserstein (GW) distance (Sturm, 2006; Mémoli, 2011) to overcome the lack of intrinsic correspondence between the distribution spaces.

GW distance can be viewed as a relaxation of Gromov-Hausdorff distance (Mémoli, 2008; Bronstein et al., 2010). It extends classical Wasserstein OT to match distributions by computing a distance between metrics defined within each of the source and target spaces. Recently, it received a high interest and has been applied to a wide set of applications, for instance in shape matching (Peyré et al., 2016; Solomon et al., 2016), unsupervised word translation (Alvarez-Melis & Jaakkola, 2018), deep learning (Bunne et al., 2019), graph partitioning and matching (Xu et al., 2019a;b) or matching weighted networks (Chowdhury & Mémoli, 2018). From a computational point view, GW distance involves a non-convex quadratic problem, hard to lift to large scale settings (Peyré & Cuturi, 2019). A remedy to a such heavy computation burden lies in a prevalent approach referred to as regularized OT (Cuturi, 2013), allowing one to add an entropic regularization penalty to the original problem. (Peyré et al., 2016) proposed the entropic GW discrepancy, that can be solved by Sinkhorn iterations (Cuturi, 2013; Benamou et al., 2015).

A major bottleneck of OT in its traditional formulation is

¹IRISA, Univ. Bretagne-Sud, IRISA, Vannes, France ²LITIS EA 4108, Univ. Rouen Normandy, Rouen, France ³LITIS EA 4108, INSA Rouen Normandy, Rouen, France. Correspondence to: Laetitia Chapel <laetitia.chapel@irisa.fr>.

that it requires the two input measures to have the same total mass. This is too restrictive for many applications since mass changes may occur due to a creation or an annihilation while computing an OT. To tackle this limitation, one may employ strategies such as *partial* or *unbalanced transport* (Guittet, 2002; Figalli, 2010; Caffarelli & McCann, 2010). Chizat et al. (2018) proposed to relax the marginal constraints of unbalanced total masses using divergences such Kullback-Leibler or total variation, allowing to use generalized Sinkhorn iterations. Yang & Uhler (2019) generalize this approach to GANs and (Lee et al., 2019) present an ADMM algorithm for the relaxed partial OT. Most of all these approaches concentrate only on partial Wasserstein (partial-W) OT.

Contributions. To the best of our knowledge, this paper is the first to deal with partial Gromov-Wasserstein (partial-GW). Our approach relies on a Frank-Wolfe optimization algorithm (Frank & Wolfe, 1956) that involves computations of partial-W. Standard strategies for computing such partial-W require relaxations of the marginals constraints. We build our approach upon adding *virtual* or *dummy* points onto the marginals (Caffarelli & McCann, 2010). These points are used as a buffer when comparing distributions with different masses, allowing the partial-W to boil down to solving an extended but classical Wasserstein problem. The main advantage of this approach is that it leads to compute exact GW distances instead of regularized GW discrepancies obtained by running Sinkhorn algorithms.

Tackling partial-GW problems that preserve sparsity of the resulting transport plan is motivated by the fact that they are more suitable to some applications such as the Positive-Unlabeled (PU) learning (Elkan & Noto, 2008; Bekker & Davis, 2018b; Du Plessis et al., 2014; Kato et al., 2019) we target in this paper. We shall notice that this is the first application of OT for solving PU learning tasks. In a nutshell, PU classification is a variant of binary classification problem, in which we have only access to labeled samples from positive (**P**) class in the training stage. The aim is to assign classes to the points of an unlabeled (**U**) set which mixes data from both positive (**P**) and negative (**N**) classes. Regarding PU learning with an OT point of view, we address the following questions:

- Is partial-W distance suited to the PU learning context when the positives and unlabeled positives samples are drawn independently from the same distributions?
- Is partial-GW distance efficient for PU learning when the source and target samples are collected under different conditions (Fig. 1, middle)?

The paper is organized as follows: we first recall some background on OT. In Section 3, we propose a Frank-Wolfe based algorithm to compute the partial-GW OT solution.

After describing in more details the PU learning task and the use of partial-OT to solve it, we illustrate the advantage of partial-GW when the source and the target distributions are collected onto distinct environments. We finally conclude and give some perspectives.

Notations In the following, bold lowercase symbols indicate vectors, bold uppercase symbols matrices and scalars in italic lowercase symbols. Σ_N is an histogram of N bins with $\{\mathbf{p} \in \mathbb{R}_+^N, \sum_i p_i = 1\}$ and δ is the Dirac function. Let $\mathbb{1}_n$ be the n -dimensional vector of ones. $\langle \cdot, \cdot \rangle_F$ stands for the Frobenius dot product

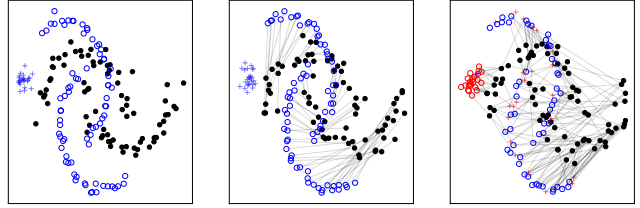


Figure 1. (Left) Source (in black) and target (in blue) distributions that have been collected under distinct environments. The source domain contains only positive points (o) whereas the target domain contains both positives and negatives (+) (Middle) Partial-GW recovers the correct labels of the unlabeled samples, with a consistent transportation plan (gray lines) (Right) Partial-W fails to assign of the labels in such context, red symbols indicating wrong assignments.

2. Background on optimal transport

Suppose we are given two point clouds $\mathcal{X} = \{\mathbf{x}_i\}_{i=1}^n$ and $\mathcal{Y} = \{\mathbf{y}_j\}_{j=1}^m$ representing source and target samples, respectively. We assume two empirical distributions $(\mathbf{p}, \mathbf{q}) \in \Sigma_n \times \Sigma_m$ over \mathcal{X} and \mathcal{Y} , that is

$$\mathbf{p} = \sum_{i=1}^n p_i \delta_{\mathbf{x}_i} \quad \text{and} \quad \mathbf{q} = \sum_{j=1}^m q_j \delta_{\mathbf{y}_j},$$

where Σ_n and Σ_m are histograms of n and m bins respectively. The set of all admissible couplings $\Pi(\mathbf{p}, \mathbf{q})$ between histograms is given by

$$\Pi(\mathbf{p}, \mathbf{q}) = \{\mathbf{T} \in \mathbb{R}_+^{n \times m} | \mathbf{T} \mathbb{1}_m = \mathbf{p}, \mathbf{T}^\top \mathbb{1}_n = \mathbf{q}\},$$

where \mathbf{T} is a coupling matrix that describes the amount of mass p_i found at \mathbf{x}_i flowing toward the mass q_j of \mathbf{y}_j .

Wasserstein and Gromov-Wasserstein distance. OT addresses the problem of optimally transporting \mathbf{p} toward \mathbf{q} , given a cost C_{ij} measured as a geometric distance between \mathbf{x}_i and \mathbf{x}_j . More precisely, its Kantorovich formulation amounts to solving the linear problem (Kantorovich, 1942)

$$\mathbf{OT}_w(\mathbf{p}, \mathbf{q}) = \min_{\mathbf{T} \in \Pi(\mathbf{p}, \mathbf{q})} \langle \mathbf{C}, \mathbf{T} \rangle_F$$

in which $\langle \cdot, \cdot \rangle_F$ stands for the Frobenius dot product. When $C = (C_{ij})_{i,j}$ is a distance matrix,

$$W_p(\mathbf{p}, \mathbf{q}) = \min_{T \in \Pi(\mathbf{p}, \mathbf{q})} \left(\sum_{i=1}^n \sum_{j=1}^m C_{ij}^p T_{ij} \right)^{\frac{1}{p}}$$

defines the p -Wasserstein distance on $\Sigma_n \times \Sigma_m$.

In some applications, the two distributions are not registered (*i.e.*, we can not compute a ground cost between \mathbf{x}_i and \mathbf{y}_j) or do not even lie in the same underlying space. Gromov-Wasserstein distance addresses this bottleneck by extending Wasserstein distance to such settings, also allowing invariance to translations, rotations or scaling. It relies on intra-domain distance matrices $C^s = (C_{ik}^s)_{i,k} = (C^s(\mathbf{x}_i, \mathbf{x}_k))_{i,k} \in \mathbb{R}_+^{n \times n}$ and $C^t = (C_{jl}^t)_{j,l} = (C^t(\mathbf{y}_j, \mathbf{y}_l))_{j,l} \in \mathbb{R}_+^{m \times m}$ that describe the distance between the points inside source and target domains and is defined as in (Mémoli, 2011):

$$GW_p(\mathbf{p}, \mathbf{q}) = \frac{1}{2} \min_{T \in \Pi(\mathbf{p}, \mathbf{q})} \left(\sum_{i,k=1}^n \sum_{j,l=1}^m (C_{ik}^s - C_{jl}^t)^p T_{ij} T_{kl} \right)^{\frac{1}{p}}$$

Entropic regularization of W- and GW-distances. In order to introduce some smoothness on the transport matrix and to speed up the computation, Cuturi (2013) considers an entropic approximation of Wasserstein distance, solving the following optimization problem:

$$\text{OT}_w^\epsilon(\mathbf{p}, \mathbf{q}) = \min_{T \in \Pi(\mathbf{p}, \mathbf{q})} \langle C, T \rangle_F + \epsilon H(T)$$

where $H(T) = -\sum_{i,j} T_{ij} \log(T_{ij})$ is the entropy of T and $\epsilon > 0$ is a regularization parameter. Note that the solution is not a distance anymore as it does not satisfy $W_p(\mathbf{p}, \mathbf{p}) = 0$. The same strategy has been used for computing GW discrepancies (Peyré et al., 2016).

Partial Wasserstein distance. The previous OT distances require the two distributions to have the same total mass $\|\mathbf{p}\|_1 = \|\mathbf{q}\|_1$. This may be a problematic assumption where some mass variation or partial mass displacement should be handled. In particular, the partial OT problem focuses on transporting only a fraction $s \leq \min(\|\mathbf{p}\|_1, \|\mathbf{q}\|_1)$ of the mass as cheaply as possible. In that case, the set of admissible couplings becomes

$$\Pi^u(\mathbf{p}, \mathbf{q}) = \{T \in \mathbb{R}_+^{n \times m} | T \mathbb{1}_m \leq \mathbf{p}, T^\top \mathbb{1}_n \leq \mathbf{q}, \mathbb{1}_n^\top T \mathbb{1}_m = s\},$$

and the partial-W distance reads as

$$W_p^u(\mathbf{p}, \mathbf{q}) = \min_{T \in \Pi^u(\mathbf{p}, \mathbf{q})} \left(\sum_{i=1}^n \sum_{j=1}^m C_{ij}^p T_{ij} \right)^{\frac{1}{p}}.$$

This problem has been studied by (Caffarelli & McCann, 2010; Figalli, 2010); numerical solutions has notably been provided by (Chizat et al., 2018) in the entropic-regularized Wasserstein case. In this paper, we rely on the (Caffarelli & McCann, 2010) strategy to solve the problem, that is described hereafter. We suppose that the total mass of each distribution is upper-bounded by a positive constant and is scaled such that $\|\mathbf{p}\|_1 \leq 1$ and $\|\mathbf{q}\|_1 \leq 1$. We add *dummy* or *virtual* points \mathbf{x}_{n+1} and \mathbf{y}_{m+1} with features at infinity and extend the cost matrix accordingly. Note that if the source or the target distribution has mass equal to 1, we do not add virtual point to its support. As such, when the mass of these dummy points is set such that $\|\mathbf{p}\|_1 * \|\mathbf{q}\|_1 = s$, computing partial-W distance boils down to solving a normalized one:

$$W_p(\tilde{\mathbf{p}}, \tilde{\mathbf{q}}) = \min_{T \in \Pi(\tilde{\mathbf{p}}, \tilde{\mathbf{q}})} \left(\sum_{i=1}^{(n+1)} \sum_{j=1}^{(m+1)} (\tilde{C}_{ij})^p T_{ij} \right)^{\frac{1}{p}}$$

where $\tilde{\mathbf{p}} = [\mathbf{p}, 1 - \|\mathbf{p}\|_1]$, $\tilde{\mathbf{q}} = [\mathbf{q}, 1 - \|\mathbf{q}\|_1]$ and

$$\tilde{C} = \begin{bmatrix} C & \Delta \\ \Delta^\top & 0 \end{bmatrix} \quad (1)$$

in which Δ is a vector containing large values. We then have the following result that expresses the difference between this extended OT with dummy points and the partial-W:

Proposition 1 Assume that $\Delta = \xi \mathbf{1}$, for some $\xi \geq \frac{1}{2} \max_{i,j} C_{ij}$, then one has

$$W_p(\tilde{\mathbf{p}}, \tilde{\mathbf{q}}) - W_p^u(\mathbf{p}, \mathbf{q}) = (2 - \|\mathbf{p}\|_1 - \|\mathbf{q}\|_1) \xi.$$

Proposition 1 can be understood as an equivalence between the extended Wasserstein and the partial-W distances, namely if one calculates an optimum \tilde{T} of $W_p(\tilde{\mathbf{p}}, \tilde{\mathbf{q}})$ we can reconstruct an optimum T of the partial Wasserstein problem and vice versa. The proof is postponed to Appendix A.1.

3. Partial Gromov-Wasserstein distance

We are interested in the partial extension of Gromov-Wasserstein transportation problem. In the case of a quadratic cost, $p = 2$, the partial-GW problem writes as

$$GW_2^u(\mathbf{p}, \mathbf{q}) = \min_{T \in \Pi^u(\mathbf{p}, \mathbf{q})} \mathcal{J}_{C^s, C^t}(T)$$

where

$$\mathcal{J}_{C^s, C^t}(T) := \frac{1}{2} \sum_{i,k=1}^n \sum_{j,l=1}^m (C_{ik}^s - C_{jl}^t)^2 T_{ij} T_{kl}. \quad (2)$$

This loss function \mathcal{J}_{C^s, C^t} is non-convex and the couplings feasibility domain $\Pi^u(\mathbf{p}, \mathbf{q})$ is convex and compact.

One may expect to introduce virtual points in the GW formulation in order to solve the partial-GW problem. Nevertheless, this workaround is no longer valid as it involves pairwise distances that do not allow the computations relative to the dummy points to be isolated (see Appendix A.2 for a detailed explanation).

In the following, we propose a solving algorithm based on Frank-Wolfe optimization scheme (Frank & Wolfe, 1956) also known as the conditional gradient method (Demyanov & Rubinov, 1970). It has recently received significant renewed interest in machine learning (Jaggi, 2013; Lacoste-Julien & Jaggi, 2015) and in OT community, since it serves as a basis to approximate penalized transport (Ferradans et al., 2013; Courty et al., 2017) or GW distances (Peyré et al., 2016; Vayer et al., 2018). Our proposed Frank-Wolfe iterations strongly rely on computing partial-W distances and as such, we can show that its solution is a sparse transport plan.

3.1. Frank-Wolfe algorithm for partial-GW

Let us first introduce some additional notations. For any tensor $\mathcal{M} = (\mathcal{M}_{ijkl})_{i,j,k,l} \in \mathbb{R}^{n \times n \times m \times m}$ and a matrix $\mathbf{T} = (T_{ij})_{i,j} \in \mathbb{R}^{n \times m}$, we denote by $\mathcal{M} \circ \mathbf{T}$ the matrix in $\mathbb{R}^{n \times m}$ such that its (i, j) -th element is defined as

$$(\mathcal{M} \circ \mathbf{T})_{i,j} = \sum_{k=1}^n \sum_{l=1}^m \mathcal{M}_{ijkl} T_{kl}$$

for all $i = 1, \dots, n, j = 1, \dots, m$. Introducing the 4-th order tensor $\mathcal{M}(\mathbf{C}^s, \mathbf{C}^t) = \frac{1}{2}((C_{ik}^s - C_{jl}^t)^2)_{i,j,k,l}$, we notice that $\mathcal{J}_{\mathbf{C}^s, \mathbf{C}^t}(\mathbf{T})$ can be written as follows

$$\mathcal{J}_{\mathbf{C}^s, \mathbf{C}^t}(\mathbf{T}) = \langle \mathcal{M}(\mathbf{C}^s, \mathbf{C}^t) \circ \mathbf{T}, \mathbf{T} \rangle_F.$$

The Frank-Wolfe algorithm for partial-GW is shown in Algorithm 1. Like classic Frank-Wolfe algorithm, it is summarized in three steps for each iteration k :

(i) compute a linear minimization oracle over the set $\Pi^u(\mathbf{p}, \mathbf{q})$, i.e.,

$$\tilde{\mathbf{T}}^{(k)} \leftarrow \underset{\mathbf{T} \in \Pi^u(\mathbf{p}, \mathbf{q})}{\operatorname{argmin}} \langle \nabla \mathcal{J}_{\mathbf{C}^s, \mathbf{C}^t}(\mathbf{T}^{(k)}), \mathbf{T} \rangle_F, \quad (3)$$

(ii) determine optimal step-size $\gamma^{(k)}$ subject to

$$\gamma^{(k)} \leftarrow \underset{\gamma \in [0,1]}{\operatorname{argmax}} \{ \mathcal{J}_{\mathbf{C}^s, \mathbf{C}^t}((1-\gamma)\mathbf{T}^{(k)} + \gamma\tilde{\mathbf{T}}^{(k)}) \}, \quad (4)$$

(iii) Update $\mathbf{T}^{(k+1)} \leftarrow (1-\gamma^{(k)})\mathbf{T}^{(k)} + \gamma^{(k)}\tilde{\mathbf{T}}^{(k)}$.

We now give more details about each step and show how this algorithm leads to a sparse transport plan.

Step (i): involving a virtual point strategy. Step (i) involves the computation of the gradient of eq. (2). Let us

denote i^* and j^* the index of the points that belong to the active set, that is to say points such that $\mathbf{T}_{i^*, \cdot} \mathbb{1}_m > 0$ or $\mathbf{T}_{\cdot, j^*}^\top \mathbb{1}_n > 0$ (elementwise), where $\mathbf{T}_{i, \cdot}$ denotes the i -th row of matrix \mathbf{T} . The associated gradient, with the matrices $(\mathbf{C}^s)^*$, $(\mathbf{C}^t)^*$ and \mathbf{T}^* computed on the active set, is given by:

$$\nabla \mathcal{J}_{(\mathbf{C}^s)^*, (\mathbf{C}^t)^*}(\mathbf{T}^*) = \mathcal{M}((\mathbf{C}^s)^*, (\mathbf{C}^t)^*) \circ \mathbf{T}^*.$$

Eq. (3) involves the full gradient matrix $\nabla \mathcal{J}_{\mathbf{C}^s, \mathbf{C}^t}(\mathbf{T})$. It can be obtained by adding missing rows and/or columns to $\nabla \mathcal{J}_{(\mathbf{C}^s)^*, (\mathbf{C}^t)^*}(\mathbf{T}^*)$ with arbitrary large and identical values α . These values should be large enough, such that those points are penalized not to be in the active set, but small enough to permit to those points to re-enter the active set. Choosing an adequate value is a difficult problem and we set it as a large quantile of the \mathbf{T}^* matrix, as advocated in (Gramfort et al., 2015). To finally solve eq. (3), we then use a virtual point strategy (see Proposition 1) and rather solve the equivalent problem

$$\underset{\mathbf{T} \in \Pi(\tilde{\mathbf{p}}, \tilde{\mathbf{q}})}{\operatorname{argmin}} \langle \tilde{\nabla} \mathcal{J}_{\mathbf{C}^s, \mathbf{C}^t}(\mathbf{T}^{(k)}), \mathbf{T} \rangle_F, \quad (5)$$

with $\tilde{\nabla} \mathcal{J}_{\mathbf{C}^s, \mathbf{C}^t}$ being $\nabla \mathcal{J}_{\mathbf{C}^s, \mathbf{C}^t}$ extended as in eq. (1). We then remove the last line and column of the resulting matrix (that is to say the ones associated to the dummy points) to get $\tilde{\mathbf{T}}^{(k)}$. Note that, instead of using this virtual point strategy, a Sinkhorn based procedure could be employed in order to get smoother transport plans.

Steps (ii) and (iii): updating $\mathbf{T}^{(k)}$. By construction, as we solve a Wasserstein problem, the solution of the step (i) is a sparse and exact optimal transport plan. Steps (ii) and (iii) involves the update of $\mathbf{T}^{(k)}$ by computing a weighted mean between the solution of step (i) $\tilde{\mathbf{T}}^{(k)}$ and the transport plan computed at the previous iteration $\mathbf{T}^{(k)}$. It can be shown that the weight $\gamma^{(k)}$ is either equal to 0 or 1 exactly, avoiding averaging of transport matrices. As both $\mathbf{T}^{(k)}$ and $\tilde{\mathbf{T}}^{(k)}$ are sparse matrices, we then guarantee that the solution obtained at each iteration is a sparse solution (see Appendix B.1 for the details of the proof).

3.2. Convergence guarantee.

Intuitively a stationary point \mathbf{T}^o for partial-GW problem verifies that every direction in the polytope with origin \mathbf{T}^o is correlated with the gradient of the loss $\mathcal{J}_{\mathbf{C}^s, \mathbf{C}^t}(\cdot)$, namely $\langle \nabla \mathcal{J}_{\mathbf{C}^s, \mathbf{C}^t}(\mathbf{T}^o); \mathbf{T} - \mathbf{T}^o \rangle_F \geq 0$ for all $\mathbf{T} \in \Pi^u(\mathbf{p}, \mathbf{q})$. A good criterion to measure distance to a stationary point at iteration k is the often used *Frank-Wolfe gap*, which is defined by

$$g_k = \langle \nabla \mathcal{J}_{\mathbf{C}^s, \mathbf{C}^t}(\mathbf{T}^{(k)}), \mathbf{T}^{(k)} - \tilde{\mathbf{T}}^{(k)} \rangle_F.$$

Note that g_k is always non-negative, and zero if and only if at a stationary point. Thanks to Theorem 1 in (Lacoste-Julien, 2016) we have

$$\min_{0 \leq k \leq K} g_k \leq \frac{\max(2J_0, L \text{diam}(\Pi^u(\mathbf{p}, \mathbf{q}))^2)}{\sqrt{K+1}},$$

where $J_0 = \mathcal{J}_{C^s, C^t}(\mathbf{T}^{(0)}) - \min_{\mathbf{T} \in \Pi^u(\mathbf{p}, \mathbf{q})} \mathcal{J}_{C^s, C^t}(\mathbf{T})$ defines the initial suboptimality, L is a Lipschitz constant of $\nabla \mathcal{J}_{C^s, C^t}$ and $\text{diam}(\Pi^u(\mathbf{p}, \mathbf{q}))$ is the $\|\cdot\|_F$ -diameter of $\Pi^u(\mathbf{p}, \mathbf{q})$ (see Appendix B.2). Therefore we can state the following lemma characterizing the convergence guarantee:

Lemma 1 *The Frank-Wolfe gap $g_K = \min_{0 \leq k \leq K} g_k$ for the partial GW loss \mathcal{J}_{C^s, C^t} after K iterations satisfies*

$$g_K \leq \frac{2 \max(J_0, \sqrt{2}s(C_{\max}^s + C_{\max}^t))}{\sqrt{K+1}} \quad (6)$$

where s is the total mass to be transported and C_{\max}^s is the maximum value of cost matrix C_{\max}^s , similarly for C^t .

Note that for the implementations, one can set $C_{\max}^s = 1 = C_{\max}^t$, hence the upper bound in (6) becomes more tight regarding a good initialization of Algorithm 1. This can be used to reduce significantly the initial suboptimality J_0 . Furthermore, according to Theorem 1 in (Lacoste-Julien, 2016), Algorithm 1 takes at most $\mathcal{O}(1/\varepsilon^2)$ iterations to find an approximate stationary point with a gap smaller than ε . Proof of Lemma 1 is given in Appendix B.2.

Algorithm 1 Frank-Wolfe algorithm for partial-GW

- 1: **Input:** Source and target samples: $(\mathcal{X}, \mathbf{p})$ and $(\mathcal{Y}, \mathbf{q})$;
 - 2: Cost matrices $C^s, p = 2, \tilde{\mathbf{p}}, \tilde{\mathbf{q}}$
 - 3: Initialize $\mathbf{T}^{(0)}$
 - 4: **for** $k = 1, 2, 3, \dots$ **do**
 - 5: // Gradient computation
 - 6: Get active set i^*, j^* and the associated $(C^s)^*, (C^t)^*$ and $(\mathbf{T}^{(k-1)})^*$
 - 7: $(\mathbf{G}^{(k)})^* \leftarrow \mathcal{M}((C^s)^*, (C^t)^*) \circ (\mathbf{T}^{(k-1)})^*$
 - 8: Construct $\mathbf{G}^{(k)}$ from $(\mathbf{G}^{(k)})^*$ by filling with α values
 - 9: // Compute partial-W OT
 - 10: Compute $\tilde{\mathbf{G}}^{(k)}$ as in eq. (1)
 - 11: $\tilde{\mathbf{T}}^{(k)} \leftarrow \text{argmin}_{\mathbf{T} \in \Pi(\tilde{\mathbf{p}}, \tilde{\mathbf{q}})} \langle \tilde{\mathbf{G}}^{(k)}, \mathbf{T} \rangle_F$
 - 12: // Line-search and update
 - 13: Compute $\gamma^{(k)}$ as in eq. (4)
 - 14: **if** $\gamma^{(k)} = 1$ **then**
 - 15: $\mathbf{T}^{(k+1)} \leftarrow \tilde{\mathbf{T}}^{(k)}$
 - 16: **else if** $\gamma^{(k)} = 0$ **then**
 - 17: $\mathbf{T}^{(k+1)} \leftarrow \mathbf{T}^{(k)}$
 - 18: **end if**
 - 19: **end for**
 - 20: **Return:** $\mathbf{T}^{(k)}$;
-

4. Optimal transport for PU learning

We hereafter investigate the application of partial optimal transport for learning from Positive and Unlabeled (PU) data. After introducing to the PU learning, we present how to adapt the formulation of partial-OT to this setting.

4.1. Overview of PU learning

Learning from PU data is a variant of classical binary classification problem, in which the training data consists of only positive data points, and the test data is composed of unlabeled positives and negatives. The term has been coined in the early 2000's and has attracted many attention as the problem arises naturally in many applications. Let $\mathbf{P} = \{\mathbf{x}_i\}_{i=1}^{n_P}$ be the positive samples drawn according to the conditional distribution $p(\mathbf{x}|\mathbf{y} = 1)$ and $\mathbf{U} = \{\mathbf{x}_i^U\}_{i=1}^{n_U}$ the unlabeled set sampled according to the marginal $p(\mathbf{x}) = \pi p(\mathbf{x}|\mathbf{y} = 1) + (1 - \pi)p(\mathbf{x}|\mathbf{y} = -1)$. The true proportion of positives, called class prior, is $\pi = p(\mathbf{y} = 1)$ and $p(\mathbf{x}|\mathbf{y} = -1)$ is the distribution of negative samples which are all unlabeled. The goal is to learn a binary classifier solely using \mathbf{P} and \mathbf{U} . A broad overview of existing approaches can be seen in (Bekker & Davis, 2018b).

Most PU learning dedicated methods commonly rely on the selected completely at random (SCAR) assumption (Elkan & Noto, 2008), which assumes that the labeled samples are drawn at random among the positive distribution, independently of their attributes. Nevertheless, this assumption is often violated in real-case scenarios and PU data are often subject to selection biases, e.g., when part of the data may be easier to obtain. Recently, a less restrictive assumption has been studied: the selected at random (SAR) setting (Bekker & Davis, 2018a) which assumes that the positives are labeled according to a subset of features of the samples. (Kato et al., 2019) move a step further and consider that the sampling scheme of the positives is such that $p(o = 1|\mathbf{x}, \mathbf{y} = 1)$ ($o = 1$ means observed label) preserves the ordering over the samples induced by the posterior distribution $p(\mathbf{y} = 1|\mathbf{x}, \mathbf{y} = 1)$. Other approaches, as in (Hsieh et al., 2019), consider a classical PU learning problem adjunct with a small proportion of observed negative samples. Those negatives are selected with bias following the distribution $p(\mathbf{x}|\mathbf{y} = -1)$.

4.2. PU learning formulation using partial OT

We propose in this paper to use partial optimal transport (either partial-W or -GW) to perform PU learning. In that context, the positive points \mathbf{P} are the source dataset \mathcal{X} and the unlabeled ones \mathbf{U} represent the target distribution \mathcal{Y} . We set the total mass s to be transported as the proportion of positives in the unlabeled set. The learned transport matrix should be such that the positive points are mapped to the

unlabeled positive samples (as they have similar features or similar intra-domain distance matrices) while the negatives are discarded (that is to say, they are mapped to the dummy point of the partial problem). When the weights of \mathbf{P} and the positive set in \mathbf{U} differ (as it is most of the time the case), the optimal transport plan is not a permutation matrix. Concretely, it means that the mass associated to a point \mathbf{x}_i^U could be splitted between some samples \mathbf{x}_i and the virtual point \mathbf{x}_{n_P+1} (see Figure 2 for an illustration). This is an undesirable scenario as it does not allow a clear identification of the negatives. Instead, we look for an optimal transport plan that belongs to the following set of couplings, in which $n = n_P, m = n_U$,

$$\Pi^{PU}(\mathbf{p}, \mathbf{q}) = \{\mathbf{T} \in \mathbb{R}_+^{n \times m} \mid \mathbf{T} \mathbf{1}_m = \mathbf{p}, \mathbf{T}^\top \mathbf{1}_n = \{\mathbf{q}, 0\}, \mathbf{1}_n^\top \mathbf{T} \mathbf{1}_m = s\},$$

that is to say that the marginals are \mathbf{q} or 0 exactly. We show in the next paragraph how this problem can be solved by introducing a group constraint on the formulation of partial-OT problem.

OT with group constraints. To consider the Wasserstein problem with a admissible constraint set $\Pi^{PU}(\mathbf{p}, \mathbf{q})$, we adopt a regularized point of view of the partial-OT problem:

$$W_p(\tilde{\mathbf{p}}, \tilde{\mathbf{q}}) = \min_{\mathbf{T} \in \Pi(\tilde{\mathbf{p}}, \tilde{\mathbf{q}})} \left(\sum_{i=1}^{(n+1)} \sum_{j=1}^{(m+1)} (\tilde{C}_{ij})^p T_{ij} \right)^{\frac{1}{p}} + \eta \Omega_C(\mathbf{T})$$

where η is a large regularization parameter and we choose $\Omega_C(\mathbf{T}) = \sum_j \sum_{cl} \|\mathbf{T}(\mathcal{I}_{cl}, j)\|_2$, where \mathcal{I}_{cl} contains the indices of the rows of \mathbf{T} that correspond to the positives or dummy points. This regularization leads to a sparse transportation map (Courty et al., 2017) and enforces each of \mathbf{U} sample to be mapped to only the \mathbf{P} samples or to the dummy point. When partial-GW is involved, we use this regularized-OT in the step (i) of the Frank-Wolfe algorithm.

Initialization of partial-W and -GW. The partial-OT computation is based on a augmented problem with a dummy point and, as such, is convex. On the contrary, the GW problem is non-convex and, although the algorithm is proved to converge, there is no guarantee that the global optimum is reached. Quality of the solution is therefore highly dependent on the initialization. We propose to rely on an initial Wasserstein barycenter problem to build a first guess of the transport matrix.

For partial-GW, as the \mathbf{C}^s and \mathbf{C}^t matrices do not lie in the same ground space, we can not define a distance function between their members. Nevertheless, within a domain, we can build two sets of “homogeneous” points. Instead of relying on a classical partitioning algorithm such as k -means, we propose to look for a barycenter with atoms

$\mathbf{U}_2 = [\mathbf{u}_2^1, \mathbf{u}_2^1]$ and weights \mathbf{b} of the set \mathbf{U} that minimizes the following function:

$$f(\mathbf{b}, \mathbf{U}_2) = W_p(\mathbf{b}, \mathbf{q}) \quad (7)$$

over the feasible sets for \mathbf{U}_2 , where $\mathbf{b} = [\pi, 1 - \pi]$. In other word, we look for the set \mathbf{U}_2 that allows having the most similar (in the Wasserstein sense) distribution \mathbf{q} than \mathbf{U} . The induced transport matrix gives then two clusters, the one with mass π serving as an initialization matrix for the GW problem.

5. Numerical experiments

In this section we illustrate partial-OT on PU applications. We describe the experimental designs and highlight how OT can be leveraged for tackling PU learning problem and the induced benefits of using partial-W or -GW in this setting.

5.1. Experimental design

We illustrate the behavior of partial-W and -GW on synthetic and real datasets in a PU learning context. First, we consider a SCAR assumption, then a SAR one and finally a more general setting, in which the underlying distributions of the point clouds come from different domains, or do not belong to the same metric space. Algorithm 1 has been implemented using the Python Optimal Transport (POT) toolbox (Flamary & Courty, 2017).

Following previous works (Kato et al., 2019; Hsieh et al., 2019), we assume that the class prior π is known throughout the experiments; otherwise, it can be estimated from $\{\mathbf{x}_i\}_{i=1}^{n_P}$ and $\{\mathbf{x}_i^U\}_{i=1}^{n_U}$ using off-the-shelf methods, e.g. (Ramaswamy et al., 2016; Plessis et al., 2017). For both partial-W and -GW, we choose $p = 2$ and the cost matrices \mathbf{C} are computed using Euclidean distance.

We carry experiments on simulated and real-world datasets under the aforementioned scenarios. We rely on six datasets Mushrooms, Shuttle, Pageblocks, USPS, Connect-4, Spambase from the UCI repository¹ (following (Kato et al., 2019)’s setting) and colored MNIST (Arjovsky et al., 2019) to illustrate our methods in SCAR and SAR settings respectively. We also consider the Caltech office dataset, which is a common application of domain adaptation (Courty et al., 2017) to explore the effectiveness of our method on heterogeneous distribution settings.

Whenever they contain several classes, these datasets are converted into a binary classification problem following (Kato et al., 2019), and the positives are the samples that belong to the $y = 1$ class. For UCI and colored MNIST datasets, we randomly draw $n_P = 400$ positive

¹<https://archive.ics.uci.edu/ml/datasets.php>

and $n_U = 800$ unlabeled points among the remaining data. As the datasets are smaller, we choose $n_P = 100$ and $n_U = 100$ for Caltech office dataset. To ease the presentation, we only report results with class prior π set as the true proportion of positive class in the dataset. We ran the experiments 10 times and report the mean accuracy rate (standard deviations are shown in Appendix C).

For the experiments, we consider unbiased PU learning method (denoted by PU in the sequel) (Du Plessis et al., 2014) and the most recent and effective method to address PU learning with a selection bias (called PUSB below) that tries to weaken the SCAR assumption (Kato et al., 2019). Whenever possible (that is to say when source and target samples share the same features), we compare our approaches P-W and P-GW with PU and PUSB; if not, we are not aware of any competitive PU learning method able to handle different features in \mathbf{P} and \mathbf{U} .

5.2. Partial Optimal Transport on a simulated dataset.

We generate the following synthetic dataset. The positive class consists of the standard entangled two moons sample and the negative class is represented by an isotropic Gaussian blob (see Fig. 1, 3).

Effect of the group constraints on the Wasserstein coupling We first draw $n_P = 10$ and $n_u = 10$ samples, 6 of them being positives. Fig. 2 shows the data and the obtained optimal couplings: enforcing a group constraint assigns some unlabeled points to the dummy point, allowing a clear identification of \mathbf{N} , whereas the solution with no such constraints may split the probability mass of the unlabeled positives between \mathbf{P} and the dummy point, preventing to consistently identify the negatives.

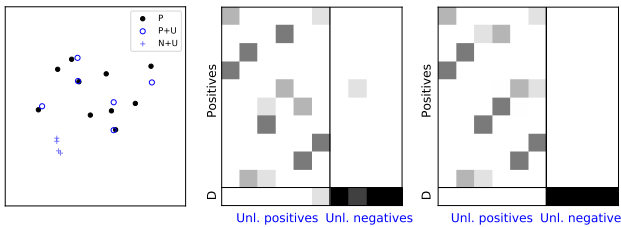


Figure 2. (Left) Positives (in black) and Unlabeled (in blue) samples (Middle) Transport matrix with no group constraints, where darker color indicates stronger matching (Right) Transport matrix with group constraints. “D” indicates the dummy point.

Partial-GW based solution. We consider different settings: (i) the distributions of \mathbf{P} and of the positives in \mathbf{U} are similar, (ii) the underlying samples of \mathbf{U} are shifted and rotated (iii) $p(\mathbf{x}|o = 1, y = 1)$ is over 3-dimensional space (by adding a third dimension drawn according to a normal distribution) and the \mathbf{U} data are 2-dimensional. In each

case, we draw $n_P = 75$ positive samples and $n_U = 100$ unlabeled data, among which 75 are positives. Partial GW allows a correct identification of \mathbf{N} in all settings (see Fig. 1, middle, and Fig. 3) where as Wasserstein-based metrics (see Fig. 1, right) fail to capture them when there is a shift in the distribution, and can not be applied when the spaces of the features are not registered.

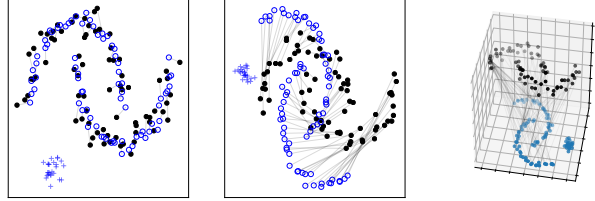


Figure 3. Positives (black) and Unlabeled (blue) data, together with the matching (in gray) that is obtained when (Left) the positives are drawn according to the same distribution (Middle) there is a shift in the positive distribution (Right) the positives $\mathbf{x} \in \mathbb{R}^3$ and the unlabeled samples are $\mathbf{x}^U \in \mathbb{R}^2$.

5.3. Partial-W and partial-GW in a PU learning under a SCAR assumption

Under SCAR, the \mathbf{P} dataset and the positives in \mathbf{U} are assumed independently and identically drawn according to the distribution $p(\mathbf{x}|o = 1, y = 1)$ from a set of positive points.

We experiment on the UCI datasets and Tab. 1 (top) summarizes our findings. As can be seen, except for Connect-4, partial-W consistently outperforms PU and PUSB under a SCAR assumption. Partial-GW has competitive results, showing that relying on intra-domain matrices may allow discriminating the classes. It nevertheless under-performs partial-W since the distributions $p(\mathbf{x}|o = 1, y = 1)$, $p(\mathbf{x}|o = 0, y = 1)$ are the same, rendering the distance matrix \mathbf{C} between \mathbf{P} and \mathbf{U} more informative.

5.4. Experiments under a SAR assumption

The SAR assumption supposes that \mathbf{P} is drawn according to the features of the samples. To implement such a setting, we inspire from (Arjovsky et al., 2019) and we construct a colored version of MNIST: each digit is colored, either in green or red, with a probability of 90% to be colored in red. The probability to label a digit $y = 1$ as positive depends on its color, with only green $y = 1$ composing the positive set. The \mathbf{U} dataset is then mostly composed of red digits.

Results under this setting are provided in Table 1 (middle). As an interesting finding, when we consider a SCAR scenario, partial-W exhibits the best performance. However, its effectiveness highly drops when a covariate shift appears in the distributions $p(\mathbf{x}|o = 1, y = 1)$ and $p(\mathbf{x}|o = 0, y = 1)$ as in this SAR scenario. On the opposite, partial-GW allows

Table 1. Average accuracy rates on various data sets with their associated priors π . Best values are indicated boldface.

DATA SET	$\pi(\%)$	PU	PUSB	P-W	P-GW
MUSHROOMS	51.8	88.7	89.0	94.8	94.0
SHUTTLE	78.6	91.0	91.9	96.5	93.3
PAGEBLOCKS	89.8	90.6	89.9	92.2	91.2
USPS	16.7	95.1	94.8	97.7	94.8
CONNECT-4	65.8	65.5	57.6	60.4	56.5
SPAMBASE	39.4	84.0	83.8	87.3	81
ORIGINAL MNIST	10	89.3	82.8	99.1	96.3
COLOR MNIST	10	87.0	80.0	86.5	96.5
SURF C \rightarrow SURF C	10	89.3	89.4	82.3	86.4
SURF C \rightarrow SURF A	10	87.7	85.6	82.2	87.2
SURF C \rightarrow SURF W	10	84.4	80.5	80.8	89.0
SURF C \rightarrow SURF D	10	82.0	83.2	80.2	94.2
DECAF C \rightarrow DECAF C	10	93.9	94.8	83.8	85.8
DECAF C \rightarrow DECAF A	10	80.5	82.2	83.8	88.6
DECAF C \rightarrow DECAF W	10	82.4	83.8	87.0	90.8
DECAF C \rightarrow DECAF D	10	82.6	83.6	84.8	95.2

maintaining a same level of accuracy as the discriminative information are preserved in intra-domain distance matrices.

5.5. Partial-W and partial-GW in a PU learning with different domains and/or feature spaces

To further validate the proposed method in a different scenarios, we apply partial-GW to a domain adaptation task. We consider the caltech office dataset, that consists of four domains: Caltech 256 (C) (Griffin et al., 2007), Amazon (A), Webcam (W) and DSLR (D) (Saenko et al., 2010). There exists a high inter-domain variability as the objects may face different illumination, orientation etc. Following a standard protocol, each image of each domain is described by a set of SURF features (Saenko et al., 2010) consisting of a normalized 800-bins histogram and by a set of DECAF features (Donahue et al., 2014), that are 4096-dimensional features extracted from a neural network. Caltech 256 represents the source domain. The unlabeled samples are formed of the Amazon, Webcam, DSLR images together with the Caltech 256 images that are not included in the positives. We perform a PCA to project the data onto $d = 10$ dimensions for the SURF features and $d = 40$ for the DECAF features. We first investigate the case where the objects are represented by SURF features but belong to the same or different domains. Results are given in Table 1 (bottom).

Considering the SURF features, we first notice that PU and PUSB outperform Partial-W and -GW when the domains are the same, and more slightly when the domains are closed (both Caltech and Amazon represent images with no background). As soon as the two domains differ more as for Webcam and DSLR (the images have a background), partial-GW exhibits the best performances, suggesting that it is able

Table 2. Average accuracy rates on domain adaptation scenarios described by different features.

SCENARIO	*=C	*=A	*=W	*=D
SURF C \rightarrow DECAF *	88.0	95.0	93.2	95.0
DECAF C \rightarrow SURF *	87.4	87.4	86.6	94.0

to capture the domain shift. Similar conclusions hold when considering the DECAF features, except that Partial-GW exhibits the best performances in all cases but one. We then consider a scenario where the objects are described by different features (Tab. 2). In that case, only partial-GW is applicable and exhibits similar performances than scenario where the features belong to the same feature space, suggesting that it is able to efficiently leverage on the discriminative information conveyed in the intra-domain similarity matrices. Namely, considering SURF C \rightarrow DECAF * (resp. DECAF C \rightarrow SURF *) gives similar performances than DECAF C \rightarrow DECAF * (resp. SURF C \rightarrow SURF *).

6. Conclusion and future work

The contributions of this work are twofold. We first propose an algorithm to compute a partial-GW distance. We show that extending the problem with dummy points (as it can be done when computing partial-W) does not lead to accurate solution. We then propose an algorithm relying on iterations of Frank-Wolfe method. Each iteration requires solving a partial-W problem. We establish that the involved line-search parameter restricts to $\{0, 1\}$, ensuring the solution sparsity. The second contribution relates to using partial-W and -GW distances to solve PU learning problems. We show that those distances compete and often outperform the state-of-the-art PU learning methods, and that partial-GW allows remarkable improvements when the underlying spaces of \mathbf{P} and \mathbf{U} are distinct or even unregistered.

While considering only features (with partial-OT) or intra-domain distances (with partial-GW), this work can be extended to define a partial-Fused Gromov-Wasserstein distance (Vayer et al., 2018) that can combines both aspects. Another line of work will also focus on lowering the computational complexity by using *sliced* partial-GW, building on existing works on *sliced* partial-W (Bonnel & Coeurjolly, 2019) and *sliced* GW (Titouan et al., 2019). Regarding the application view point, we envision a potential use of the approach to subgraph matching (Kriege & Mutzel, 2012) or PU learning on graphs (Zhao et al., 2011) as GW has been proved to be effective to compare structured data such as graphs. Finally, we plan to derive an extension of this work to PU learning in which the proportion of positives in the dataset will be estimated in a unified optimal transport formulation, building on results of GW-based test of isomorphism between distributions (Br  cheteau, 2019).

References

- Alvarez-Melis, D. and Jaakkola, T. Gromov-Wasserstein alignment of word embedding spaces. In *Proceedings of the 2018 Conference on Empirical Methods in Natural Language Processing*, pp. 1881–1890, 2018.
- Arjovsky, M., Chintala, S., and Bottou, L. Wasserstein Generative Adversarial Networks. In *Proceedings of the 34th International Conference on Machine Learning*, volume 70, pp. 214–223, 2017.
- Arjovsky, M., Bottou, L., Gulrajani, I., and Lopez-Paz, D. Invariant risk minimization. *arXiv preprint arXiv:1907.02893*, 2019.
- Bekker, J. and Davis, J. Learning from positive and unlabeled data under the selected at random assumption. In *Proceedings of Machine Learning Research*, volume 94, pp. 8–22, 2018a.
- Bekker, J. and Davis, J. Learning from positive and unlabeled data: A survey. Technical report, arXiv preprint [arXiv:1811.04820](https://arxiv.org/abs/1811.04820), 2018b.
- Benamou, J. D., Carlier, G., Cuturi, M., Nenna, L., and Peyré, G. Iterative Bregman projections for regularized transportation problems. *SIAM J. Scientific Computing*, 37, 2015.
- Bonneel, N. and Coeurjolly, D. Spot: sliced partial optimal transport. *ACM Transactions on Graphics (TOG)*, 38(4): 1–13, 2019.
- Bonneel, N., Van de Panne, M., Paris, S., and Heidrich, W. Displacement interpolation using lagrangian mass transport. *ACM Trans. Graph.*, 30(6):158:1–12, 2011.
- Bréchet, C. A statistical test of isomorphism between metric-measure spaces using the distance-to-a-measure signature. *Electronic Journal of Statistics*, 13(1):795–849, 2019.
- Bronstein, A. M., Bronstein, M. M., Kimmel, R., Mahmoudi, M., and Sapiro, G. A Gromov-Hausdorff framework with diffusion geometry for topologically-robust non-rigid shape matching. *International Journal of Computer Vision*, 89(2-3):266–286, 2010.
- Bunne, C., Alvarez-Melis, D., Krause, A., and Jegelka, S. Learning generative models across incomparable spaces. In *Proceedings of the 36th International Conference on Machine Learning*, volume 97, pp. 851–861, 2019.
- Caffarelli, L. A. and McCann, R. J. Free boundaries in optimal transport and monge-ampère obstacle problems. *Annals of Mathematics*, 171(2):673–730, 2010.
- Chizat, L., Peyré, G., Schmitzer, B., and Vialard, F.-X. Scaling algorithms for unbalanced optimal transport problems. *Math. Comput.*, 87:2563–2609, 2018.
- Chowdhury, S. and Mémoli, F. The Gromov-Wasserstein distance between networks and stable network invariants. *CoRR*, abs/1808.04337, 2018.
- Courty, N., Flamary, R., Tuia, D., and Rakotomamonjy, A. Optimal transport for domain adaptation. *IEEE transactions on pattern analysis and machine intelligence*, 39(9): 1853–1865, 2017.
- Cuturi, M. Sinkhorn distances: Lightspeed computation of optimal transport. In *Advances in Neural Information Processing Systems* 26, pp. 2292–2300, 2013.
- Demyanov, V. F. and Rubinov, A. M. Approximate methods in optimization problems. *Elsevier Publishing Company*, 53, 1970.
- Donahue, J., Jia, Y., Vinyals, O., Hoffman, J., Zhang, N., Tzeng, E., and Darrell, T. Decaf: A deep convolutional activation feature for generic visual recognition. In *International conference on machine learning*, pp. 647–655, 2014.
- Du Plessis, M. C., Niu, G., and Sugiyama, M. Analysis of learning from positive and unlabeled data. In *Advances in neural information processing systems*, pp. 703–711, 2014.
- Elkan, C. and Noto, K. Learning classifiers from only positive and unlabeled data. In *Proceedings of the 14th ACM SIGKDD international conference on Knowledge discovery and data mining*, pp. 213–220, 2008.
- Ferradans, S., Papadakis, N., Rabin, J., Peyré, G., and Aujol, J. F. Regularized discrete optimal transport. In Kuijper, A., Bredies, K., Pock, T., and Bischof, H. (eds.), *Scale Space and Variational Methods in Computer Vision*, pp. 428–439, Berlin, Heidelberg, 2013. Springer Berlin Heidelberg.
- Figalli, A. The optimal partial transport problem. *Archive for Rational Mechanics and Analysis*, 195(2):533–560, 2010.
- Flamary, R. and Courty, N. Pot python optimal transport library. <https://github.com/rflamary/POT>, 2017.
- Frank, M. and Wolfe, P. An algorithm for quadratic programming. *Naval Research Logistics Quarterly*, 3(1-2): 95–110, 1956.
- Gramfort, A., Peyré, G., and Cuturi, M. Fast optimal transport averaging of neuroimaging data. In Ourselin, S., Alexander, D. C., Westin, C.-F., and Cardoso, M. J. (eds.),

- Information Processing in Medical Imaging*, pp. 261–272, Cham, 2015. Springer International Publishing.
- Griffin, G., Holub, A., and Perona, P. Caltech-256 object category dataset. Technical report, California Institute of Technology, 2007.
- Guittet, K. Extended kantorovich norms: a tool for optimization. *Tech. Rep. 4402*, 2002.
- Ho, N., Nguyen, X. L., Yurochkin, M., Bui, H. H., Huynh, V., and Phung, D. Multilevel clustering via wasserstein means. In *Proceedings of the 34th International Conference on Machine Learning - Volume 70*, pp. 1501–1509, 2017.
- Hsieh, Y., Niu, G., and Sugiyama, M. Classification from positive, unlabeled and biased negative data. In *Proceedings of the 36th International Conference on Machine Learning*, volume 97, 2019.
- Jaggi, M. Revisiting Frank-Wolfe: Projection-free sparse convex optimization. In *Proceedings of the 30th International Conference on Machine Learning*, number 1, pp. 427–435, 2013.
- Kantorovich, L. On the transfer of masses (in Russian). *Doklady Akademii Nauk*, 2:227–229, 1942.
- Kato, M., Teshima, T., and Honda, J. Learning from positive and unlabeled data with a selection bias. In *ICLR*, 2019.
- Kriege, N. and Mutzel, P. Subgraph matching kernels for attributed graphs. In *Proceedings of the 29th International Conference on Machine Learning*, 2012.
- Lacoste-Julien, S. Convergence rate of Frank-Wolfe for non-convex objectives. *CoRR*, abs/1607.00345, 2016.
- Lacoste-Julien, S. and Jaggi, M. On the global linear convergence of frank-wolfe optimization variants. *Neural Information Processing Systems 2015*, pp. 496–504, 2015.
- Lee, J., Bertrand, N., and Rozell, C. Parallel unbalanced optimal transport regularization for large scale imaging problems. Technical report, arXiv preprint [arXiv:1909.00149](https://arxiv.org/abs/1909.00149), 2019. Under review.
- Memoli, F. Gromov-hausdorff distances in euclidean spaces. In *2008 IEEE Computer Society Conference on Computer Vision and Pattern Recognition Workshops*, pp. 1–8, June 2008.
- Mémoli, F. Gromov–Wasserstein distances and the metric approach to object matching. *Foundations of Computational Mathematics*, 11(4):417–487, 2011.
- Monge, G. Mémoire sur la théorie des déblais et des remblais. *Histoire de l’Académie Royale des Sciences*, pp. 666–704, 1781.
- Peyré, G. and Cuturi, M. Computational optimal transport. *Foundations and Trends® in Machine Learning*, 11(5-6): 355–607, 2019.
- Peyré, G., Cuturi, M., and Solomon, J. Gromov-Wasserstein averaging of kernel and distance matrices. In *Proceedings of the 33rd International Conference on Machine Learning - Volume 48*, pp. 2664–2672, 2016.
- Plessis, M. C., Niu, G., and Sugiyama, M. Class-prior estimation for learning from positive and unlabeled data. *Mach. Learn.*, 106(4):463–492, April 2017.
- Ramaswamy, H., Scott, C., and Tewari, A. Mixture proportion estimation via kernel embeddings of distributions. In *International Conference on Machine Learning*, pp. 2052–2060, 2016.
- Saenko, K., Kulis, B., Fritz, M., and Darrell, T. Adapting visual category models to new domains. In *European conference on computer vision*, pp. 213–226, 2010.
- Solomon, J., de Goes, F., Peyré, G., Cuturi, M., Butscher, A., Nguyen, A., Du, T., and Guibas, L. Convolutional wasserstein distances: Efficient optimal transportation on geometric domains. *ACM Trans. Graph.*, 34(4):66:1–66:11, 2015.
- Solomon, J., Peyré, G., Kim, V. G., and Sra, S. Entropic metric alignment for correspondence problems. *ACM Trans. Graph.*, 35(4):72:1–13, 2016.
- Sturm, K. T. On the geometry of metric measure spaces. *Acta Math.*, 196(1):133–177, 2006.
- Titouan, V., Flamary, R., Courty, N., Tavenard, R., and Chapel, L. Sliced gromov-wasserstein. In *Advances in Neural Information Processing Systems 32*, pp. 14726–14736. Curran Associates, Inc., 2019.
- Vayer, T., Chapel, L., Flamary, R., Tavenard, R., and Courty, N. Fused gromov-wasserstein distance for structured objects: theoretical foundations and mathematical properties. *CoRR*, abs/1811.02834, 2018.
- Villani, C. *Optimal Transport: Old and New*, volume 338. Springer Berlin Heidelberg, 2009.
- Xu, H., Luo, D., and Carin, L. Scalable Gromov-Wasserstein learning for graph partitioning and matching. In *Advances in Neural Information Processing Systems 32*, pp. 3046–3056, 2019a.
- Xu, H., Luo, D., Zha, H., and Carin, L. Gromov-Wasserstein learning for graph matching and node embedding. In *Proceedings of the 36th International Conference on Machine Learning*, 2019b.

Yang, K. D. and Uhler, C. Scalable unbalanced optimal transport using generative adversarial networks. In *International Conference on Learning Representations*, 2019.

Zhao, Y., Kong, X., and Philip, S. Y. Positive and unlabeled learning for graph classification. In *2011 IEEE 11th International Conference on Data Mining*, pp. 962–971. IEEE, 2011.

A. Partial Optimal Transport with dummy points

A.1. Proof of Proposition 1: equivalence between partial-W and balanced extended Wasserstein optimums

We note

$$\mathbf{OT}_{\text{uw}}(\mathbf{p}, \mathbf{q}) = \min_{\mathbf{T} \in \Pi^u(\mathbf{p}, \mathbf{q})} \langle \mathbf{C}, \mathbf{T} \rangle_F,$$

and

$$\mathbf{OT}_w(\tilde{\mathbf{p}}, \tilde{\mathbf{q}}) = \min_{\mathbf{T} \in \Pi(\tilde{\mathbf{p}}, \tilde{\mathbf{q}})} \langle \tilde{\mathbf{C}}, \mathbf{T} \rangle_F.$$

Step 1. We first show that for every admissible plan $\tilde{\mathbf{T}} \in \mathbb{R}^{(n+1) \times (m+1)}$ for $\mathbf{OT}_w(\tilde{\mathbf{p}}, \tilde{\mathbf{q}})$ there exists $\mathbf{T}^u \in \mathbb{R}^{n \times m}$ an admissible transport plan for $\mathbf{OT}_{\text{uw}}(\mathbf{p}, \mathbf{q})$. Towards this goal, let us define $\mathbf{T}^u = (T_{ij}^u)_{i,j}$ such that $T_{ij}^u = \tilde{T}_{ij}$, for all $i \in \{1, \dots, n\}$ and $j \in \{1, \dots, m\}$. We after show that using this construction \mathbf{T}^u belongs to the admissible points of $\mathbf{OT}_{\text{uw}}(\mathbf{p}, \mathbf{q})$ by just checking its marginal inequality conditions, namely $\mathbf{T}^u \mathbb{1}_m \leq \mathbf{p}$ and $\mathbf{T}^{u\top} \mathbb{1}_n \leq \mathbf{q}$.

We have

$$\begin{aligned} \sum_{j=1}^m T_{ij}^u &= \sum_{j=1}^m \tilde{T}_{ij} = \tilde{p}_i = p_i, \forall i = 1, \dots, n, \\ \sum_{i=1}^n T_{ij}^u &= \sum_{i=1}^n \tilde{T}_{ij} = \tilde{q}_j = q_j, \forall j = 1, \dots, m. \end{aligned}$$

Now let us verify the cost function. Splitting the total cost $\langle \tilde{\mathbf{C}}, \tilde{\mathbf{T}} \rangle_F$ into four parts we get

$$\begin{aligned} \sum_i^{n+1} \sum_j^{m+1} \tilde{C}_{ij} \tilde{T}_{ij} &= \sum_{i,j}^{n,m} \tilde{C}_{ij} \tilde{T}_{ij} + \sum_{i=1}^{n+1} \tilde{C}_{i(m+1)} \tilde{T}_{i(m+1)} \\ &\quad + \sum_{j=1}^{m+1} \tilde{C}_{(n+1)j} \tilde{T}_{(n+1)j} + \tilde{C}_{(n+1)(m+1)} \tilde{T}_{(n+1)(m+1)} \\ &= \sum_{i,j}^{n,m} C_{ij} T_{ij}^u + (2 - \|\mathbf{p}\|_1 - \|\mathbf{q}\|_1) \xi, \end{aligned}$$

where in the last equation we use: $\tilde{C}_{i,m+1} = \tilde{C}_{n+1,j} = \xi$ for all $i \in \{1, \dots, n\}$ and $j \in \{1, \dots, m\}$, and $\sum_{j=1}^{m+1} \tilde{T}_{(n+1)j} = \tilde{p}_{n+1} = 1 - \|\mathbf{p}\|_1$ and $\sum_{i=1}^{n+1} \tilde{T}_{i(m+1)} = \tilde{q}_{m+1} = 1 - \|\mathbf{q}\|_1$. Hence

$$\mathbf{OT}_w(\tilde{\mathbf{p}}, \tilde{\mathbf{q}}) - \mathbf{OT}_{\text{uw}}(\mathbf{p}, \mathbf{q}) = (2 - \|\mathbf{p}\|_1 - \|\mathbf{q}\|_1) \xi.$$

Step 2. Now we will construct a transport plan $\tilde{\mathbf{T}}$ from \mathbf{T}^u . Let us define

$$\begin{cases} \tilde{T}_{ij} = T_{ij}^u, & \text{for } i = 1, \dots, n; j = 1, \dots, m, \\ \tilde{T}_{i,m+1} = p_i - \sum_{j=1}^m T_{ij}^u, & \text{for } i = 1, \dots, n, \\ \tilde{T}_{n+1,j} = q_j - \sum_{i=1}^n T_{ij}^u, & \text{for } j = 1, \dots, m, \\ \tilde{T}_{n+1,m+1} = 1 - \|\mathbf{p}\|_1 - \|\mathbf{q}\|_1 + \sum_{i,j=1}^{n,m} T_{ij}^u. \end{cases}$$

We have $\tilde{T} \geq 0$ since T^u satisfies the constraints $T^u \mathbf{1}_n \leq \mathbf{p}$ and $T^{u\top} \mathbf{1}_m \leq \mathbf{q}$. Let then calculate the marginals from \tilde{T} . For a fixed $i \in \{1, \dots, n\}$ we have

$$\begin{aligned} \sum_{j=1}^{m+1} \tilde{T}_{ij} &= \sum_{j=1}^m \tilde{T}_{ij} + \tilde{T}_{i(m+1)} \\ &= \sum_{j=1}^m T_{ij}^u + p_i - \sum_{j=1}^m T_{ij}^u \\ &= p_i \\ &= \tilde{p}_i, \end{aligned}$$

and

$$\begin{aligned} \sum_{j=1}^{m+1} \tilde{T}_{(n+1)j} &= \sum_{j=1}^m \tilde{T}_{(n+1)j} + \tilde{T}_{(n+1)(m+1)} \\ &= \sum_{j=1}^m (q_j - \sum_{i=1}^n T_{ij}^u) + 1 - \|\mathbf{p}\|_1 - \|\mathbf{q}\|_1 + \sum_{i,j=1}^{n,m} T_{ij}^u \\ &= 1 - \|\mathbf{p}\|_1 \\ &= \tilde{p}_{n+1}. \end{aligned}$$

Similarly, one can verify that $\sum_{j=1}^{m+1} \tilde{T}_{ij} = \tilde{q}_j$ for all $j = 1, \dots, m$. Moreover, it is easy to show that the total mass of \tilde{T} is equal to 1, i.e. $\sum_{i,j}^{n+1,m+1} \tilde{T}_{ij} = 1$. Analogously, we can calculate the cost function by splitting it into four parts as was done before to get

$$\mathbf{OT}_w(\tilde{\mathbf{p}}, \tilde{\mathbf{q}}) - \mathbf{OT}_{uw}(\mathbf{p}, \mathbf{q}) = (2 - \|\mathbf{p}\|_1 - \|\mathbf{q}\|_1)\xi.$$

A.2. Partial Gromov-Wasserstein with dummy points does not work

While solving the partial-W problem can be straightforwardly achieved by adding dummy points (and extend the cost matrix C) to the problem, the same strategy does not hold for GW (by extending their intra-cost matrices C^s and C^t in the same way, as its formulation involves pairs of points and the loss associated to the dummy point is not constant. Indeed:

$$\begin{aligned} T^* &= \underset{T \in \Pi(\mathbf{p}^u, \mathbf{q}^u)}{\operatorname{argmin}} \sum_{i,k=1}^n \sum_{j,l=1}^m (C_{ik}^t - C_{jl}^s)^p T_{ij} T_{kl} \\ &\quad + (\star) \end{aligned}$$

where

$$\begin{aligned} (\star) &= \sum_{j,l=1}^m \left(2 \sum_k^n (\xi - C_{jl}^s)^p T_{(n+1)j} T_{kl} \right. \\ &\quad \left. + 2(C_{jl}^s)^p T_{(n+1)j} T_{(n+1)l} \right) \\ &\quad + \sum_{i,k=1}^n \left(2 \sum_j^m (C_{ik}^t - \xi)^p T_{i,j} T_{k(m+1)} \right. \\ &\quad \left. + 2(C_{ik}^t)^p T_{i(m+1)} T_{k(m+1)} \right) \\ &\quad + 0 \end{aligned}$$

depends on the C^s and C^t values.

B. Details of Frank-Wolfe algorithm for partial-GW

B.1. Line-search

The step size in the line-search of Frank-Wolfe algorithm for partial-GW is given by

$$\gamma_{\max}^{(k)} \leftarrow \underset{\gamma \in [0,1]}{\operatorname{argmax}} \{ \mathcal{J}_{C^s, C^t} \left((1 - \gamma)T^{(k)} + \gamma\tilde{T}^{(k)} \right) \}.$$

In the following we prove that for each Frank-Wolfe iteration k in our setting, $\gamma^{(k)} \in \{0, 1\}$. To proceed in this direction, let us define $\mathbf{E}^{(k)} = \tilde{T}^{(k)} - T^{(k)}$ and the function $\phi : [0, 1] \rightarrow \mathbb{R}$ such that

$$\phi(\gamma^{(k)}) = \mathcal{J}_{C^s, C^t}(T^{(k)} + \gamma \mathbf{E}^{(k)}).$$

Straightforwardly, one has

$$\begin{aligned} \phi(\gamma) &= \langle \mathcal{M}(C^s, C^t) \circ (T^{(k)} + \gamma \mathbf{E}^{(k)}), T^{(k)} + \gamma \mathbf{E}^{(k)} \rangle_F \\ &= \langle \mathcal{M}(C^s, C^t) \circ T^{(k)}, T^{(k)} \rangle_F \\ &\quad + \gamma \langle \mathcal{M}(C^s, C^t) \circ T^{(k)}, \mathbf{E}^{(k)} \rangle_F \\ &\quad + \gamma \langle \mathcal{M}(C^s, C^t) \circ \mathbf{E}^{(k)}, T^{(k)} \rangle_F \\ &\quad + \gamma^2 \langle \mathcal{M}(C^s, C^t) \circ \mathbf{E}^{(k)}, \mathbf{E}^{(k)} \rangle_F. \end{aligned}$$

Since we choose a quadratic cost, $p = 2$, then for any T, R one has

$$\langle \mathcal{M}(C^s, C^t) \circ R, T \rangle_F = \langle \mathcal{M}(C^s, C^t) \circ T, R \rangle_F. \quad (8)$$

Thanks to the property (8), we get

$$\begin{aligned} \phi(\gamma) &= \gamma^2 \langle \mathcal{M}(C^s, C^t) \circ \mathbf{E}^{(k)}, \mathbf{E}^{(k)} \rangle_F \\ &\quad + 2\gamma \langle \mathcal{M}(C^s, C^t) \circ \mathbf{E}^{(k)}, T^{(k)} \rangle_F \\ &\quad + \langle \mathcal{M}(C^s, C^t) \circ T^{(k)}, T^{(k)} \rangle_F. \end{aligned}$$

This yields that its derivative is given by

$$\begin{aligned} \phi'(\gamma) &= 2\gamma \langle \mathcal{M}(C^s, C^t) \circ \mathbf{E}^{(k)}, \mathbf{E}^{(k)} \rangle_F \\ &\quad + 2 \langle \mathcal{M}(C^s, C^t) \circ \mathbf{E}^{(k)}, T^{(k)} \rangle_F. \end{aligned}$$

Hence the extremum $\gamma_o^{(k)}$ of $\phi(\gamma^{(k)})$ is attained at

$$\gamma_o^{(k)} = -\frac{\langle \mathcal{M}(\mathbf{C}^s, \mathbf{C}^t) \circ \mathbf{E}^{(k)}, \mathbf{T}^{(k)} \rangle_F}{\langle \mathcal{M}(\mathbf{C}^s, \mathbf{C}^t) \circ \mathbf{E}^{(k)}, \mathbf{E}^{(k)} \rangle_F},$$

Since $\mathbf{T}^{(k)} = \tilde{\mathbf{T}}^{(k)} - \mathbf{E}^{(k)}$, we get

$$\gamma_o^{(k)} = 1 - \frac{\langle \mathcal{M}(\mathbf{C}^s, \mathbf{C}^t) \circ \mathbf{E}^{(k)}, \tilde{\mathbf{T}}^{(k)} \rangle_F}{\langle \mathcal{M}(\mathbf{C}^s, \mathbf{C}^t) \circ \mathbf{E}^{(k)}, \mathbf{E}^{(k)} \rangle_F}.$$

On the other hand, we have

$$\begin{aligned} \langle \mathcal{M}(\mathbf{C}^s, \mathbf{C}^t) \circ \mathbf{E}^{(k)}, \mathbf{E}^{(k)} \rangle_F \\ = \langle \mathcal{M}(\mathbf{C}^s, \mathbf{C}^t) \circ \tilde{\mathbf{T}}^{(k)}, \tilde{\mathbf{T}}^{(k)} \rangle_F \\ + \langle \mathcal{M}(\mathbf{C}^s, \mathbf{C}^t) \circ \mathbf{T}^{(k)}, \mathbf{T}^{(k)} \rangle_F \\ - 2\langle \mathcal{M}(\mathbf{C}^s, \mathbf{C}^t) \circ \mathbf{T}^{(k)}, \tilde{\mathbf{T}}^{(k)} \rangle_F. \end{aligned}$$

Recall that a $\tilde{\mathbf{T}}^{(k)}$ is an optimum transport plan for the cost $\nabla \mathcal{J}_{\mathbf{C}^s, \mathbf{C}^t}(\mathbf{T}^{(k)}) = \mathcal{M}(\mathbf{C}^s, \mathbf{C}^t) \circ \mathbf{T}^{(k)}$, i.e.

$$\tilde{\mathbf{T}}^{(k)} = \mathbf{O}\mathbf{T}_w(\mathbf{p}, \mathbf{q}) \quad (9)$$

with a ground matrix $\mathcal{M}(\mathbf{C}^s, \mathbf{C}^t) \circ \mathbf{T}^{(k)}$. Taking into account (9) and the fact that $\mathbf{T}^{(k)} \in \Pi(\mathbf{p}, \mathbf{q})$, we get

$$\begin{aligned} \langle \mathcal{M}(\mathbf{C}^s, \mathbf{C}^t) \circ \mathbf{T}^{(k)}, \tilde{\mathbf{T}}^{(k)} \rangle_F \\ \leq \langle \mathcal{M}(\mathbf{C}^s, \mathbf{C}^t) \circ \mathbf{T}^{(k)}, \mathbf{T}^{(k)} \rangle_F. \end{aligned}$$

Therefore,

$$\begin{aligned} \langle \mathcal{M}(\mathbf{C}^s, \mathbf{C}^t) \circ \mathbf{E}^{(k)}, \mathbf{E}^{(k)} \rangle_F \\ \geq \langle \mathcal{M}(\mathbf{C}^s, \mathbf{C}^t) \circ \tilde{\mathbf{T}}^{(k)}, \tilde{\mathbf{T}}^{(k)} \rangle_F \\ - \langle \mathcal{M}(\mathbf{C}^s, \mathbf{C}^t) \circ \mathbf{T}^{(k)}, \tilde{\mathbf{T}}^{(k)} \rangle_F, \end{aligned}$$

equivalently

$$\begin{aligned} \langle \mathcal{M}(\mathbf{C}^s, \mathbf{C}^t) \circ \mathbf{E}^{(k)}, \mathbf{E}^{(k)} \rangle_F \\ \geq \langle \mathcal{M}(\mathbf{C}^s, \mathbf{C}^t) \circ \mathbf{E}^{(k)}, \tilde{\mathbf{T}}^{(k)} \rangle_F. \end{aligned}$$

Setting $a^{(k)} = \langle \mathcal{M}(\mathbf{C}^s, \mathbf{C}^t) \circ \mathbf{E}^{(k)}, \mathbf{E}^{(k)} \rangle_F$ and $b^{(k)} = \langle \mathcal{M}(\mathbf{C}^s, \mathbf{C}^t) \circ \mathbf{E}^{(k)}, \tilde{\mathbf{T}}^{(k)} \rangle_F$, we have $\gamma_o^{(k)} = 1 - \frac{b^{(k)}}{a^{(k)}}$.

Remark that the set of optimums $\{\gamma_o^{(k)}\}$ depends on the signs of $a^{(k)}$ and $b^{(k)}$. In the following we summarize all the cases.

- If $a^{(k)} < 0$, gives $\frac{b^{(k)}}{a^{(k)}} > 1$, then the function ϕ is increasing on $[0, 1]$, which gives $\{\gamma_o^{(k)} \text{ optimum}\} = \emptyset$.
- If $a^{(k)} > 0$, then we have $\gamma_o^{(k)} \leq 1$ iff $b^{(k)} \geq 0$. In this case ϕ is decreasing on $[0, \gamma_o^{(k)}]$ and increasing in $[\gamma_o^{(k)}, 1]$.

- If $a^{(k)} > 0$, we have $\gamma_o^{(k)} \geq 1$ iff $b^{(k)} \leq 0$, and in this case ϕ is decreasing on $[0, 1]$, and $\{\gamma_o^{(k)} \text{ optimum}\} = \emptyset$.

Finally the parameter $\gamma_{\max}^{(k)}$ in the line-search step of Frank-Wolfe algorithm for partial GW verifies

$$\gamma_{\max}^{(k)} = \begin{cases} 1, & \text{if } a^{(k)} < 0 \\ 1, & \text{if } a^{(k)} > 0 \text{ and } b^{(k)} \geq 0 \\ 0, & \text{if } a^{(k)} > 0 \text{ and } b^{(k)} \leq 0. \end{cases}$$

B.2. Guarantee of convergence: Proof of Lemma 1

Let us first calculate the diameter of the couplings set $\Pi^u(\mathbf{p}, \mathbf{q})$ with respect to the Frobenius norm $\|\cdot\|_F$. One has

$$\text{diam}(\Pi^u(\mathbf{p}, \mathbf{q})) = \sup_{(\mathbf{T}, \mathbf{Q}) \in \Pi^u(\mathbf{p}, \mathbf{q})^2} \|\mathbf{T} - \mathbf{Q}\|_F.$$

Using triangle inequality and the fact that T_{ij}, Q_{ij} are probability masses that is $T_{ij}, Q_{ij} \in [0, 1]$, we get

$$\begin{aligned} \|\mathbf{T} - \mathbf{Q}\|_F^2 &\leq 2\|\mathbf{T}\|_F^2 + 2\|\mathbf{Q}\|_F^2 \\ &\leq 2 \sum_{i,j}^{n,m} T_{ij}^2 + 2 \sum_{i,j}^{n,m} Q_{ij}^2 \\ &\leq 2 \sum_{i,j}^{n,m} T_{ij} + 2 \sum_{i,j}^{n,m} Q_{ij} \\ &\leq 4s \end{aligned}$$

where s is the total mass to be transported. Thus

$$\text{diam}(\Pi^u(\mathbf{p}, \mathbf{q})) \leq 2\sqrt{s}.$$

For the Lipschitz constant of the gradient of $\mathcal{J}_{\mathbf{C}^s, \mathbf{C}^t}$ we proceed as follows: for any $\mathbf{T}, \mathbf{Q} \in \Pi^u(\mathbf{p}, \mathbf{q})$ we have

$$\begin{aligned} \|\nabla \mathcal{J}_{\mathbf{C}^s, \mathbf{C}^t}(\mathbf{T}) - \nabla \mathcal{J}_{\mathbf{C}^s, \mathbf{C}^t}(\mathbf{Q})\|_F^2 \\ = \sum_{i,j}^{n,m} \left(\sum_{k,l}^{n,m} \mathcal{M}_{ijkl} (T_{kl} - Q_{kl}) \right)^2 \\ \leq \sup_{i,j,k,l} \mathcal{M}_{ijkl}^2 \sum_{i,j}^{n,m} \left(\sum_{k,l}^{n,m} (T_{kl} - Q_{kl}) \right)^2 \\ \leq 4 \sup_{i,j,k,l} \mathcal{M}_{ijkl}^2 \|\mathbf{T} - \mathbf{Q}\|_F^2. \end{aligned}$$

We have also

$$\begin{aligned} \sup_{i,j,k,l} \mathcal{M}_{ijkl}^2 &= \frac{1}{4} \sup_{i,j,k,l} (C_{ik}^s - C_{jl}^s)^2 \\ &\leq \frac{1}{2} ((\mathbf{C}_{\max}^s)^2 + (\mathbf{C}_{\max}^t)^2). \end{aligned}$$

Hence the Lipschitz constant of $\nabla \mathcal{J}_{\mathbf{C}^s, \mathbf{C}^t}(\cdot)$ verifies $L \leq \sqrt{2}(\mathbf{C}_{\max}^s + \mathbf{C}_{\max}^t)$. This gives the desired result.

C. Additional table

Table 3. Standard deviation of accuracy rates on different datasets and scenarios.

DATASET/SCENARIO	PU	PUSB	P-W	P-GW
MUSHROOMS	0.014	0.019	0.007	0.015
SHUTTLE	0.028	0.038	0.016	0.011
PAGEBLOCKS	0.026	0.022	0.010	0.014
USPS	0.012	0.015	0.003	0.008
CONNECT-4	0.006	0.020	0.013	0.017
SPAMBASE	0.031	0.035	0.011	0.072
ORIGINAL MNIST	0.030	0.034	0.005	0.007
COLORLED MNIST	0.035	0.034	0.010	0.011
SURF C→SURF C	0.019	0.015	0.011	0.012
SURF C→SURF A	0.014	0.018	0.034	0.030
SURF C→SURF W	0.010	0.064	0.039	0.016
SURF C→SURF D	0.006	0.036	0.048	0.011
DECAF C→DECAF C	0.022	0.017	0.016	0.008
DECAF C→DECAF A	0.019	0.022	0.021	0.011
DECAF C→DECAF W	0.030	0.009	0.016	0.026
DECAF C→DECAF D	0.033	0.008	0.016	0.013
SURF C→DECAF C	-	-	-	0.006
SURF C→DECAF A	-	-	-	0.006
SURF C→DECAF W	-	-	-	0.022
SURF C→DECAF D	-	-	-	0.010
DECAF C→SURF C	-	-	-	0.009
DECAF C→SURF A	-	-	-	0.018
DECAF C→SURF W	-	-	-	0.016
DECAF C→SURF D	-	-	-	0.037